Fundus Autofluorescence and Spectral-Domain Optical Coherence Tomography Characteristics in a Rapidly Progressing Form of Geographic Atrophy

Monika Fleckenstein,[1] *Steffen Schmitz-Valckenberg,*[1] *Christine Martens,*[1] *Sebastian Kosanetzky,*[1] *Christian K. Brinkmann,*[1] *Gregory S. Hageman,*[2] *and Frank G. Holz*[1]

Purpose. To further characterize a previously described phenotypic variant of geographic atrophy (GA) associated with rapid progression and a diffuse-trickling appearance on fundus autofluorescence (FAF).

Methods. Thirty-six patients (60 eyes; 72.2% women; mean age, 69.4 ± 10.7 years) with this distinct phenotype were examined by simultaneous confocal scanning laser ophthalmoscopy (cSLO) and spectral-domain optical coherence tomography (SD-OCT) imaging. Images were qualitatively and quantitatively analyzed and compared with 60 eyes (38 patients) with non diffuse-trickling GA.

Results. The atrophic area in the diffuse-trickling phenotype showed a grayish FAF signal and characteristic coalescent lobular configuration at the lesion boundaries. SD-OCT revealed a marked splitting of band 4 (the presumptive retinal pigment epithelium (RPE)/Bruch's membrane (BM) complex) in all 240 analyzed border sections of diffuse-trickling GA eyes (four borders/eye) with a mean distance between the inner and outer parts of band 4 of 23.2 ± 7.5μm. This finding was present in only 13.8% (33/240) of analyzed border sections in non diffuse-trickling GA.

Conclusions. Patients with the rapidly progressing diffuse-trickling GA phenotype exhibited a characteristic marked separation within the RPE/BM complex on SD-OCT-imaging. The presumed histopathologic correlates are basal laminar deposits. Such deposits may promote RPE cell death and, thus, contribute to rapid GA progression. The persistence of these deposits within the atrophic lesion may account for the distinct grayish FAF appearance, which differs from the markedly reduced signal in other forms of GA. Identification of such alterations based on FAF and SD-OCT imaging may be helpful in future interventional trials directed toward slowing GA progression. (ClinicalTrials.gov number, NCT00393692.) (*Invest Ophthalmol Vis Sci.* 2011;52:3761–3766) DOI:10.1167/iovs.10-7021

Geographic atrophy (GA), a late-stage manifestation of various complex and monogenetic retinal diseases including age-related macular degeneration (AMD), is characterized by loss of the retinal pigment epithelium (RPE), photoreceptor cells, and the choriocapillaris layer. Although AMD is one of the most well-characterized late-onset, complex trait diseases with aberrant function of the complement system playing a key role in GA pathogenesis,[1–4] the molecular pathways of GA in the context of AMD remain poorly understood. For example, it is not known at what anatomic level (i.e., photoreceptors, RPE, Bruch's membrane, or choriocapillaris) the initiating event occurs. It is likely that different pathogenic mechanisms lead to the common downstream pathogenetic pathway—that is, outer retinal atrophy in the context of AMD.

Recent developments in retinal imaging technologies have allowed for refined phenotyping in retinal diseases.[5,6] In particular, fundus autofluorescence (FAF) has been useful in the characterization of GA caused by AMD, Stargardt's disease, and other macular or diffuse retinal dystrophies.[7–10] With the advent of optical coherence tomography (OCT), cross-sectional analyses of the human retina are possible in vivo. Subsequently, spectral-domain (SD)-OCT technology has been introduced, with further improvements in imaging speed and resolution compared with previous time-domain OCT imaging technology.[11–13] By applying this new technology, a considerable spectrum of morphologic alterations in GA has been described.[14–20]

We recently classified various patterns of abnormal FAF in eyes with GA based on confocal scanning laser ophthalmoscopy (cSLO) FAF imaging. One phenotype, described as diffuse-trickling, is characterized by a distinct lobular atrophy with a grayish FAF appearance.[10] Of note, this phenotype showed the highest progression rate over time (median, 3.02 mm^2/year) even when compared with other relatively rapidly progressing GA subtypes (median, 1.87 mm^2/year; $P = 0.001$).[10] This observation was confirmed by the recently published GAP study data, reporting a progression rate of 3.48 mm^2/year for this distinct phenotype (Holz FG, et al. *IOVS* ARVO E-Abstract 2010;51:94). The specific pathogenic mechanisms that distinguish this GA subtype, however, are unknown. The aim of the present study was to further characterize this distinct FAF phenotype using simultaneous cSLO and high-resolution SD-OCT imaging.

From the [1]Department of Ophthalmology, University of Bonn, Bonn, Germany; and the [2]John A. Moran Eye Center, Department of Ophthalmology and Visual Sciences, University of Utah, Salt Lake City, Utah.

Supported by the German Research Council Research Priority Program in Age-Related Macular Degeneration Grant SPP 1088, Ho 1926/1-3 (FGH); a German Society of Ophthalmology research grant (MF); BONFOR Program Grant O-137-0012 (Faculty of Medicine, University of Bonn) (MF); National Institutes of Health Grant R24 EY017404 (GSH); and an unrestricted grant to the University of Utah John A. Moran Eye Center and the Department of Ophthalmology and Visual Sciences from Research to Prevent Blindness, Inc.

Submitted for publication December 8, 2010; revised January 6, 2011; accepted January 12, 2011.

Disclosure: **M. Fleckenstein**, Heidelberg Engineering (F, C); **S. Schmitz-Valckenberg**, Heidelberg Engineering (F, C, R); **C. Martens**, Heidelberg Engineering (F); **S. Kosanetzky**, Heidelberg Engineering (F); **C.K. Brinkmann**, Heidelberg Engineering (F, C); **G.S. Hageman**, None; **F.G. Holz**, Heidelberg Engineering (F, C, R)

Corresponding author: Frank G. Holz, Department of Ophthalmology, University of Bonn, Ernst-Abbe-Strasse 2, D-53127 Bonn, Germany; frank.holz@ukb.uni-bonn.de.

Patients and Methods

Patients

The Fundus Autofluorescence in Age-Related Macular Degeneration (FAM) study database was screened for patients exhibiting the diffuse-trickling phenotype according to the classification system of abnormal FAF in the perilesional zone of GA, as introduced previously.[10] Briefly, the diffuse-trickling phenotype is characterized by coalescent lobular atrophic lesions that spread over the posterior pole (Fig. 1). In advanced stages, retinal areas outside the arcades and nasally to the optic disc may be involved. The fovea is typically spared until late in the course of the disease. With progression and subsequent foveal involvement, visual acuity often drops to hand motions within months of disease onset. The atrophic area appears grayish rather than dark black, with the latter phenomenon of marked reduction in the FAF signal intensity typically seen in areas of atrophy with other GA subtypes. FAF intensity adjacent to the atrophic lobules is markedly enhanced with a diffuse trickling of the FAF signal toward the periphery. A reticular background pattern (reticular pseudodrusen) is also observed frequently.

A comparable sample size of patients with non diffuse-trickling GA was analyzed in the FAM study to compare FAF and SD-OCT changes. Inclusion criteria in the FAM study included age greater than 50 years and the presence of GA in at least one eye as a result of AMD (for details, see Holz et al.[10]). Each patient underwent a routine ophthalmologic examination, including determination of best-corrected visual acuity. A standardized case report form including ophthalmologic history, possible risk factors, and family history was completed for each patient. The study followed the tenets of the Declaration of Helsinki, and informed consent was obtained from each patient.

Image Acquisition

Pupils were dilated with 1.0% tropicamide and 2.5% phenylephrine before retinal imaging. Imaging was carried out with an instrument (Spectralis HRA+OCT; Heidelberg Engineering, Heidelberg, Germany) that allows for simultaneous recording of cSLO and SD-OCT with two independent scanning mirrors, as described previously.[21] cSLO images were obtained according to a standardized operation protocol that includes the acquisition of near-infrared reflectance (λ = 815 nm) and FAF (excitation at λ = 488 nm, emission 500–700 nm) images.[10] The size of the field of view encompassed 30° × 30°, with an image resolution of 768 × 768 pixels. Simultaneous SD-OCT imaging was carried out with an illumination wavelength of 870 nm, an acquisition speed of 40,000 A-scans, and a scan depth of 1.8 mm. Two SD-OCT scans, one vertical and one horizontal, per eye were performed through the approximate foveal center. In eyes with GA, additional scans were performed if these central scans did not detect the atrophic lesion.

Fluorescein angiography (λ = 488 nm, emission 500–700 nm, 10% fluorescein dye) was performed when other clinical signs pointed to the coexistence of a neovascular process. Color fundus photographs were obtained with a fundus camera (FF 450 Visupac ZK5; Carl Zeiss Meditec AG, Jena, Germany).

Image Analysis: Fundus Autofluorescence and Spectral-Domain Optical Coherence Tomography

A diagnosis of diffuse-trickling was based on FAF images as described here and previously.[10] Two independent readers performed the grading; in cases of discrepancy, a third reader was consulted for arbitration.

For SD-OCT, individual bands lying below the hyporeflective band of the outer nuclear layer were identified based on recent descriptions.[22] These included the following: a thin hyperreflective band that presumably corresponds to the external limiting membrane (ELM); a slightly thicker hyperreflective band that presumably corresponds to the interface of the inner and outer segments of the photoreceptor layer (IPRL); a thin, only occasionally visible, hyperreflective band that presumably corresponds to the outer segment–RPE interdigitation; and a broad hyperreflective band that is believed to correspond to the RPE/Bruch's membrane complex (RPE/BM).

The configuration of a nasal, temporal, inferior, and superior atrophic border was analyzed in all eyes with the diffuse-trickling pheno-

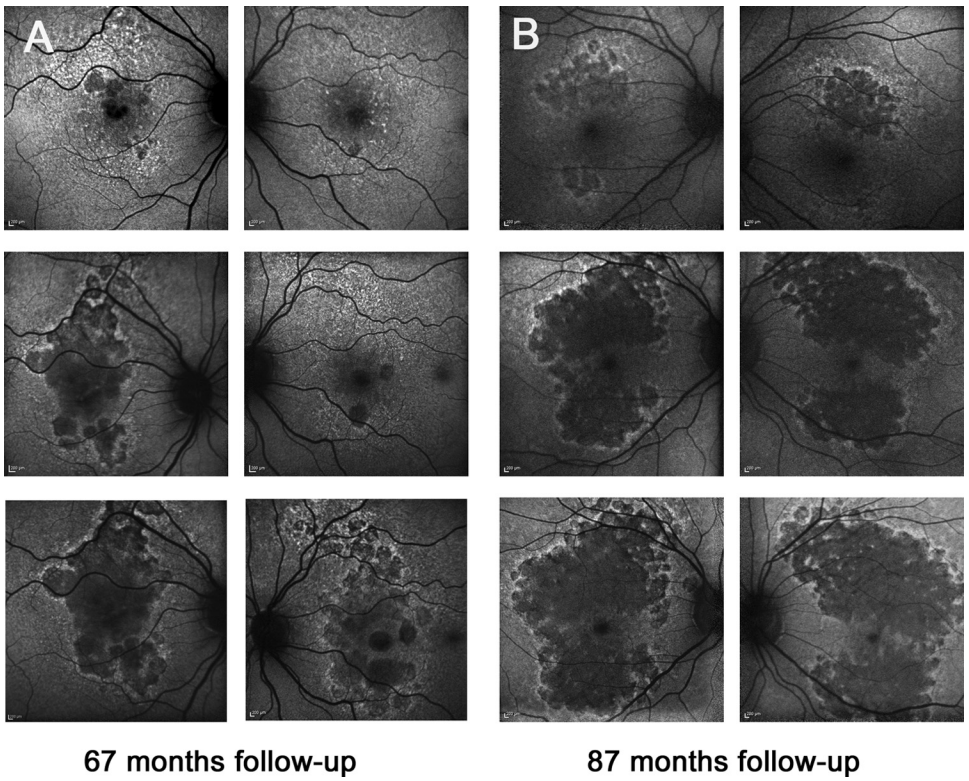

Figure 1. The diffuse-trickling phenotype in GA. Longitudinal course monitored by FAF imaging in two female study patients (**A**, 68 years of age at first examination; **B**, 53 years of age at first examination). Both exhibited rapidly progressing lobular atrophy with a grayish appearance on FAF imaging. (**A**) There is early involvement of the fovea in the right eye; the course of the disease in this patient was asymmetrical. However, after 67 months of follow-up, a large atrophic area in the left eye (similar in size to the one in the right eye) and foveal involvement were observed. (**B**) Although there were large atrophic areas, the fovea was bilaterally spared until later in the disease course.

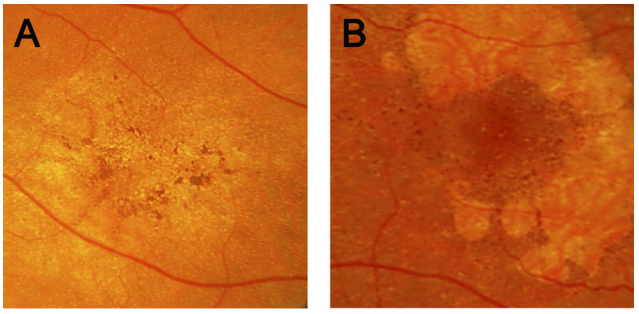

FIGURE 2. Funduscopic features of the diffuse-trickling phenotype in GA. Dense, granular, hyperpigmentary changes are often observed in the central macula and in fellow eyes without GA (**A**). The borders of the atrophic lesions appeared hyperpigmented (**B**).

type and in a comparable sample size of eyes with non diffuse-trickling GA (see Fig. 3 for the classification scheme). Two independent readers performed grading; in case of discrepancy, a third reader was consulted for arbitration.

Quantitative analyses were performed using the measuring tool of the Heidelberg Engineering software (Heidelberg Eye Explorer; Heidelberg Engineering). For measurements, the SD-OCT images were magnified twice. All statistical calculations were carried out using data mining software (SPSS, version 18; IBM, New York, NY).

RESULTS

Study Subject Characteristics

A total of 36 patients (26 [72.2%] women) with the diffuse-trickling phenotype and SD-OCT recordings was identified from the FAM study database. Twenty-four study patients (66.7%) with bilateral GA (all patients bilaterally exhibited the diffuse-trickling phenotype), three patients with GA in one eye and hyperpigmentary changes in the other eye (8.3%), and nine patients with GA in one eye and choroidal neovascularization (CNV) in the fellow eye (25%) were identified. Mean age at first examination was 69.4 ± 10.7 years.

Mean visual acuity of the eye of each subject with better acuity was logMAR 0.33 ± 0.47 (minimum logMAR 1.6, maximum logMAR 0) and for all eyes was logMAR 0.45 ± 0.5 (minimum logMAR 2.0, maximum logMAR 0). In the 60 eyes with GA, 35 (58.0%) had no foveal involvement (foveal sparing).

The comparison group consisted of 60 eyes (38 patients) with non diffuse-trickling GA; 21 [55.3%] patients were women, and the mean age at examination was 75.7 ± 7.3 years. Eyes were categorized according to the classification system of abnormal FAF in the perilesional zone of GA[10] as follows: two eyes without abnormal FAF (3.3%), two eyes with the focal FAF pattern (3.3%), four eyes with the banded pattern (6.7%), 32 eyes with diffuse-reticular/diffuse-branching FAF pattern (53.3%), 16 eyes with the diffuse-fine granular pattern (26.7%), and four eyes with the diffuse-fine granular with peripheral punctuate spots FAF pattern (6.7%).

Funduscopic Characteristics in Diffuse-Trickling Geographic Atrophy

Eyes with the diffuse-trickling FAF phenotype exhibited dense granular hyperpigmentary changes in the central macula (Figs. 2A, 2B; also seen in fellow eyes that had not developed atrophy [Fig. 2A]), and the borders of the atrophic lesions appeared hyperpigmented (Fig. 2B). Typical soft drusen are infrequent in this phenotype.

Spectral-Domain Optical Coherence Tomography Characteristics in Diffuse-Trickling Geographic Atrophy

In the 60 eyes with diffuse-trickling GA, the junctional zone between atrophy and the surrounding retina was characterized by thinning and loss of the ONL, loss of the ELM (band 1), and loss of the IPRL (band 2), as described previously in GA.[14] Two hyperreflective bands were observed (Fig. 3C), in stark contrast to previously described border types in GA[19] (Figs. 3A, 3B). The density of the innermost band disappeared at the border of GA (this was verified by comparison of simultaneous cSLO and SD-OCT images), and the outermost band remained throughout the atrophic lesion (Figs. 3, 4). These two bands seemed to result from a splitting of band 4 (assumed RPE/Bruch's membrane complex), beginning in the perilesional zone. Furthermore, there was also an obvious separation of band 4 at the posterior pole in fellow eyes without GA (three eyes with pigmentary changes [Fig. 5A] and nine eyes with CNV [Fig. 5B]).

Classification of Geographic Atrophy Borders by Spectral-Domain Optical Coherence Tomography

Four borders (nasal, temporal, inferior, and superior) in each eye with GA were classified into three categories based on the configuration of SD-OCT changes. They were type 1 and type 2 borders according to Brar et al.[19] (Figs. 3A, 3B) and the splitting border (Fig. 3C).

In eyes with diffuse-trickling GA, all 240 border zones (four borders in 60 eyes) showed an obvious separation of band 4 and were, therefore, classified as the splitting type. In eyes with non diffuse-trickling GA, the 240 borders (four borders in 60 eyes) were classified as follows: 43 type 1 borders (17.9%), 155 type 2 borders (64.6%), and 33 splitting borders (13.8%). Nine borders (3.8%) could not be classified. All 17 eyes with at least one splitting border exhibited the diffuse-reticular/diffuse-branching or the diffuse-fine granular FAF pattern.

Distance between the Innermost and Outermost Regions of Spectral-Domain Optical Coherence Tomography Band 4 in the Splitting Border Type

To quantitatively analyze the obvious splitting of band 4, the distance between the lower rim of the inner part of band 4 and

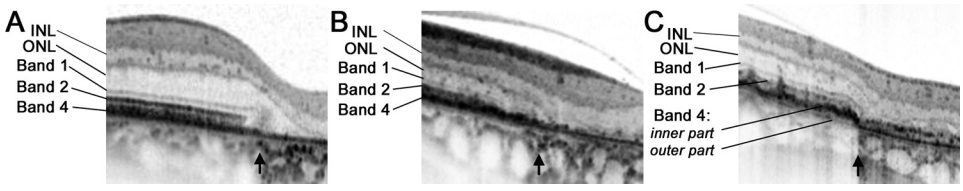

FIGURE 3. Different types of borders as visualized by SD-OCT. (**A**, **B**) GA other than diffuse-trickling phenotype. Band 4 (assumed RPE/BM complex) narrows, and an outer layer remains throughout the atrophic area (assumed Bruch's membrane). According to Brar et al.,[19] the margin depicted in (**A**) represents a type 1 border with smooth margins and no alterations of the outer retina, and the margin in (**B**) represents a type 2 border with severe alterations in the outer retinal layers and irregular margins. (**C**) In contrast to (**A**) and (**B**), the border of GA in the diffuse trickling phenotype is characterized by splitting of band 4 in inner and outer regions.

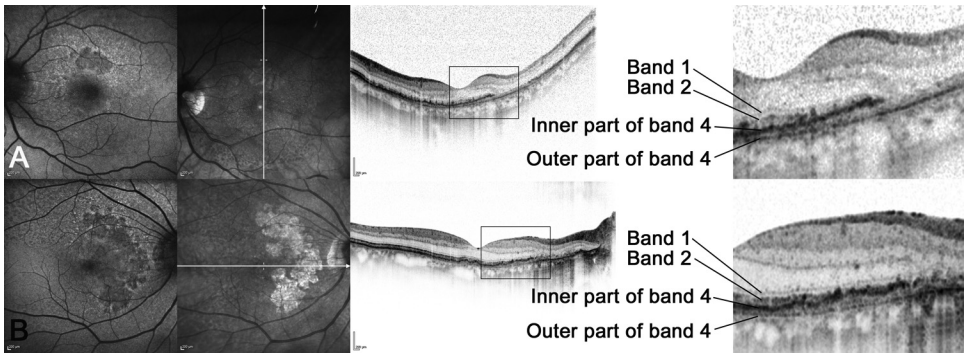

FIGURE 4. (**A**, **B**, two different patients) Diffuse-trickling GA phenotype. Fundus autofluorescence imaging, simultaneous infrared reflectance, and SD-OCT. Magnification of the SD-OCT images at the border of GA reveals an obvious splitting of SD-OCT band 4 in inner and outer regions.

the upper rim of the outer part of band 4 at a nasal, temporal, inferior, and superior border was measured at all sections with the splitting border type.

In eyes with diffuse-trickling GA, measurements could be performed in all 240 border zones. The mean distance between the innermost and outermost regions of band 4 were 23.2 ± 7.5 μm, ranging between 10 μm and 50 μm. There was no significant difference between the distances at a distinct retinal location with a mean thickness of 22.3 ± 6.6 μm nasally, 24 ± 7.5 μm temporally, 22.9 μm ± 7.4 inferiorly, or 22.7 ± 7.7 μm superiorly (Friedman-test; $P = 0.141$).

In eyes with non diffuse-trickling GA only in 5 of 33 splitting borders the distance between the two parts of band 4 was quantifiable (range, 10–50 μm). At the other 28 splitting border sections, the distance was too small for reliable quantification.

Atrophic Lesion

To further determine the possible cause of the grayish appearance of the diffuse-trickling atrophy in FAF images (Figs. 1, 4, 6 upper panel), SD-OCT alterations within the atrophic lesion were analyzed. In contrast to the black-appearing atrophic lesion of non diffuse-trickling GA (Fig. 6, top), SD-OCT imaging revealed a thin, discontinuous hyperreflective band between the inner nuclear layer (INL) and the outer part of band 4 (Fig. 6, bottom). This band appeared in elongation of the inner part of band 4 (Fig. 3C). This finding was present in all eyes with diffuse-trickling GA and was most pronounced close to the border zone.

DISCUSSION

This study demonstrates that the splitting of the SD-OCT band 4 at the posterior pole is a characteristic feature in patients exhibiting the previously described rapidly progressing diffuse-trickling phenotype based on cSLO FAF imaging. Several authors have evaluated SD-OCT alterations at the border of atrophy in GA patients.[14–20] Brar et al.[19] introduced a classification into two different border types: type 1, with smooth margins and no alterations of the outer retina (Fig. 3A), and type 2, with severe alterations in the outer retinal layers and irregular margins with or without increased optical reflectivity of the RPE (Fig. 3B). In this classification, a splitting of band 4 has not been described. In a previous study, we have shown that the separation of band 4 is one of several alterations visualized by SD-OCT.[14] Comparison of the GA border configuration in other GA phenotypes suggests that this observation was not limited to the diffuse-trickling phenotype, though it was most prominent in this GA subtype.

We speculate that the SD-OCT changes found in all eyes and in all border sections in this rapidly progressing GA variant are associated with the evolution of this GA subtype. It is widely accepted that band 4 corresponds anatomically to the RPE/Bruch's membrane complex.[22] Histologically, various AMD-associated lesions, including CNV membranes, drusen, and basal deposits, occur within this region.[23–27] Because no signs of CNV were observed in the eyes showing the diffuse-trickling FAF pattern at the time of inclusion and because the distinct SD-OCT alterations were also observed in fellow eyes with only pigmentary changes, it is unlikely that the material observed between the innermost and outermost layers of band 4 represented exudative lesions, nor would this have been a manifestation of typical soft drusen because no dome-shaped elevations were observed by SD-OCT[14,28] and no soft drusen were visualized in color fundus photographs.

The most supportable histopathologic correlate is that of basal deposits, particularly basal laminar deposits (BLamD), which occur between the RPE basement membrane and its plasma membrane.[29–31] BLamD has been identified in human donor eyes as a hallmark of AMD, particularly late-stage disease.[26,27,31–33] However, no direct clinical correlate has been described to date by funduscopy or by in vivo imaging modalities including FAF imaging.

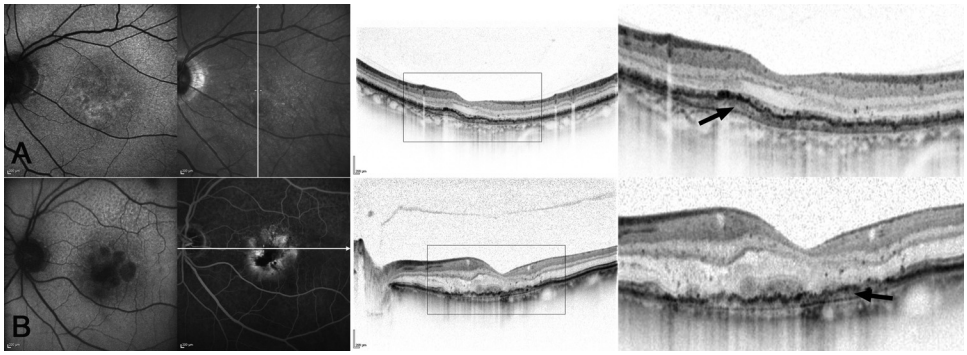

FIGURE 5. Fellow eyes of the diffuse-trickling GA phenotype. FAF, simultaneous infrared reflectance (*top*), FA (*bottom*), and SD-OCT. (**A**) Fellow eye with increased FAF signal but no GA. Magnification of the SD-OCT image reveals an obvious separation of band 4 (*arrow*). (**B**) Fellow eye with choroidal neovascularization (leakage in FA imaging and intraretinal fluid in SD-OCT imaging). Magnification of the SD-OCT image reveals an obvious separation of band 4 (*arrow*).

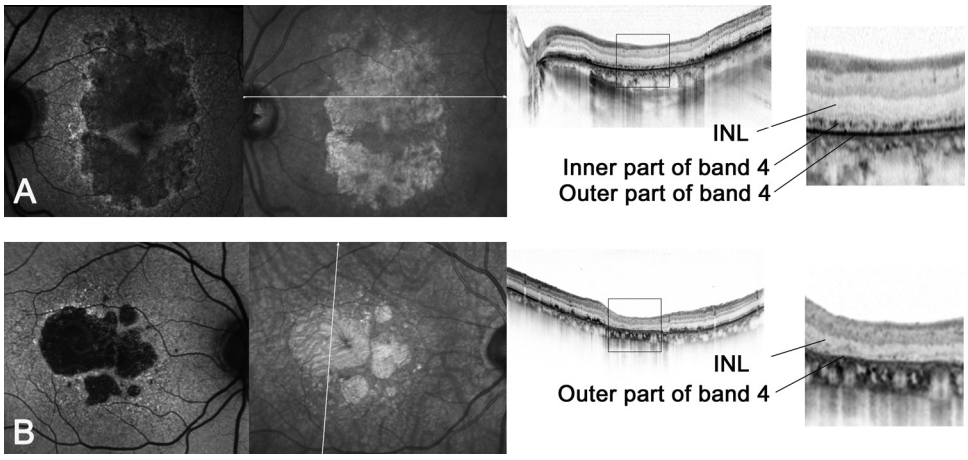

FIGURE 6. (**A**) Diffuse-trickling GA shows a coalescent lobular configuration with a grayish appearance in FAF images (*left*). SD-OCT imaging reveals a thin discontinuous hyperreflective band between the INL and the outer part of band 4 within the atrophy. (**B**) Representative example (diffuse-fine granular phenotype) for the typical black appearance of the atrophic lesion in FAF imaging in eyes with non diffuse-trickling GA (the choroidal vessels may show a slightly increased FAF signal). In SD-OCT imaging, compared with eyes with the diffuse-trickling phenotype, there was no obvious hyperreflective band between the INL and the outer part of band 4.

The observation of the persistent splitting of band 4 within atrophic areas was consistent with the postmortem finding of persistent BLamD in areas of GA itself and in disciform scars.[23] We also propose that the grayish appearance of the atrophic lesion observed on FAF imaging of this phenotype might have been attributed to the presence of basal deposits within the region of atrophy, though this remains to be proven conclusively.

Although the precise origin and nature of basal deposits, particularly BLamD, have not yet been determined, these may result from nonspecific RPE compromise secondary to ischemia, oxidative stress, or other injury or aberrant lipid trafficking.[24] Alternatively, these extracellular deposits may be the consequence of AMD-specific genes. In one clinicopathology study, Sarks et al.[24] correlated the excessive accumulation of BLamD with funduscopically visible hyperpigmentation. Based on this observation, it has been speculated that basal deposits lead by increasing thickening to separation of the RPE from the choroidal blood supply, and subsequently to RPE and photoreceptor degeneration.[24,34–37] BLamD is reported to be up to 25 μm thick ex vivo[24]; other preliminary data suggest that an even thicker BLamD layer may exist in the eyes of donors with clinical histories of GA (unpublished observation; M. Rudolf, G.S. Hageman, personal communication). Given the limited resolution of SD-OCT compared with histopathology,[21] it is conceivable that the deposition of material and the splitting of the RPE/Bruch's membrane complex may not be delineable by in vivo imaging in the mild stage. Presumably, most GA eyes exhibits BLamD, as histologic studies have suggested.[26,27,31–33] However, this phenotypic hallmark would become detectable in vivo only when a critical thickness is reached with current SD-OCT imaging technology. Therefore, we speculate that the diffuse-trickling phenotype is characterized by excessive BLamD accumulation. Both the presence of dense hyperpigmentation seen by funduscopy (which may represent hypertrophic, clustered, or migrated melanin-containing RPE cells) and the behavior with rapid atrophy progression over time of the diffuse-trickling phenotype would be in accordance with the concept that this phenotype is a GA manifestation at the severe end of the spectrum of the disease. The observation of similar findings in fellow eyes without GA suggests that this alteration represents a generalized metabolic dysfunction at the photoreceptor, RPE, Bruch's membrane, or choriocapillaris level, which may precede atrophy evolution but may also be associated with CNV development. This assumption is in accordance with the histologic findings that BLamD is not confined to GA.[26,27,31–33] Furthermore, our results do not exclude the presence of BLamD in other GA phenotypes. We found borders in non diffuse-trickling GA with clear splitting of band 4; however, this observation was less frequent than in eyes with diffuse-trickling GA. Interestingly, if present in non diffuse-trickling GA, the splitting border was found in other rapidly progressing GA subtypes (diffuse-reticular/diffuse-branching and diffuse-fine granular),[10] but in most border sections the distance between the two layers of band 4 was too small for quantification.

Limitations of this study include the merely descriptive character of in vivo SD-OCT changes. There is as yet no direct histologic correlation between characteristic SD-OCT findings and histologic characteristics. Therefore, the possibility remains that the splitting of the SD-OCT band 4 is an imaging artifact. Nevertheless, the consistency of this finding in all eyes with the diffuse-trickling phenotype and the presence in vertical and horizontal scans within an eye, for instance, support that the splitting was due to a real morphologic alteration. However, only the Spectralis SD-OCT (Heidelberg Engineering) was used herein. Although we would assume that other SD-OCT instruments now available would visualize the diffuse deposits in a similar way, a systematic comparison is lacking. Furthermore, the exact anatomic correlation of the different SD-OCT bands is not completely understood, especially of the most outer hyperreflective bands. Therefore, we cannot conclude definitively which anatomic layers represent the inner and the outer parts of SD-OCT band 4.

Finally, the classification of SD-OCT borders was performed at only four border sections in each eye with GA. This represents a minor part of the entire border zone of the atrophic lesion. In the ongoing study, we will address the challenge of analysis strategies of SD-OCT imaging for GA phenotyping.

In conclusion, we present distinct SD-OCT and FAF features of patients with a rapidly progressing GA subtype. The most likely anatomic correlates of the alterations visualized by OCT technology are diffuse basal deposits located beneath the RPE. Excessive accumulation may accelerate RPE cell death and, therefore, GA progression.

References

1. Gehrs KM, Jackson JR, Brown EN, Allikmets R, Hageman GS. Complement, age-related macular degeneration and a vision of the future. *Arch Ophthalmol.* 2010;128:349–358.
2. Anderson DH, Radeke MJ, Gallo NB, et al. The pivotal role of the complement system in aging and age-related macular degeneration: hypothesis re-visited. *Prog Retin Eye Res.* 2010;29:95–112.
3. Baird PN, Hageman GS, Guymer RH. New era for personalized medicine: the diagnosis and management of age-related macular degeneration. *Clin Exp Ophthalmol.* 2009;37:814–821.

4. Gehrs KM, Anderson DH, Johnson LV, Hageman GS. Age-related macular degeneration—emerging pathogenetic and therapeutic concepts. *Ann Med.* 2006;38:450–471.
5. Fleckenstein M. Retinal imaging in geographic atrophy [Bildgebende Diagnostik bei Geographischer Atrophie]. *Der Ophthalmologe.* 2010;107:1007–1015.
6. Schmitz-Valckenberg S, Holz FG. [Geographic atrophy in AMD]. *Ophthalmologe*. 2010;107:1016–1019.
7. Bindewald A, Schmitz-Valckenberg S, Jorzik JJ, et al. Classification of abnormal fundus autofluorescence patterns in the junctional zone of geographic atrophy in patients with age related macular degeneration. *Br J Ophthalmol.* 2005;89:874–878.
8. von Ruckmann A, Fitzke FW, Bird AC. In vivo fundus autofluorescence in macular dystrophies. *Arch Ophthalmol.* 1997;115:609–615.
9. Boon CJ, Klevering BJ, Cremers FP, et al. Central areolar choroidal dystrophy. *Ophthalmology.* 2009;116:771–782, 782 e771.
10. Holz FG, Bindewald-Wittich A, Fleckenstein M, Dreyhaupt J, Scholl HP, Schmitz-Valckenberg S. Progression of geographic atrophy and impact of fundus autofluorescence patterns in age-related macular degeneration. *Am J Ophthalmol.* 2007;143:463–472.
11. de Boer JF, Cense B, Park BH, Pierce MC, Tearney GJ, Bouma BE. Improved signal-to-noise ratio in spectral-domain compared with time-domain optical coherence tomography. *Opt Lett.* 2003;28:2067–2069.
12. Wojtkowski M, Srinivasan V, Ko T, Fujimoto J, Kowalczyk A, Duker J. Ultrahigh-resolution, high-speed, Fourier domain optical coherence tomography and methods for dispersion compensation. *Opt Express.* 2004;12:2404–2422.
13. Drexler W. Ultrahigh-resolution optical coherence tomography. *J Biomed Opt.* 2004;9:47–74.
14. Fleckenstein M, Charbel Issa P, Helb HM, et al. High-resolution spectral domain-OCT imaging in geographic atrophy associated with age-related macular degeneration. *Invest Ophthalmol Vis Sci.* 2008;49:4137–4144.
15. Wolf-Schnurrbusch UE, Enzmann V, Brinkmann CK, Wolf S. Morphologic changes in patients with geographic atrophy assessed with a novel spectral OCT-SLO combination. *Invest Ophthalmol Vis Sci.* 2008;49:3095–3099.
16. Schmitz-Valckenberg S, Fleckenstein M, Helb HM, Charbel Issa P, Scholl HP, Holz FG. In vivo imaging of foveal sparing in geographic atrophy secondary to age-related macular degeneration. *Invest Ophthalmol Vis Sci.* 2009;50:3915–3921.
17. Lujan BJ, Rosenfeld PJ, Gregori G, et al. Spectral domain optical coherence tomographic imaging of geographic atrophy. *Ophthalmic Surg Lasers Imaging.* 2009;40:96–101.
18. Bearelly S, Chau FY, Koreishi A, Stinnett SS, Izatt JA, Toth CA. Spectral domain optical coherence tomography imaging of geographic atrophy margins. *Ophthalmology.* 2009;116:1762–1769.
19. Brar M, Kozak I, Cheng L, et al. Correlation between spectral-domain optical coherence tomography and fundus autofluorescence at the margins of geographic atrophy. *Am J Ophthalmol.* 2009;148:439–444.
20. Fleckenstein M, Schmitz-Valckenberg S, Adrion C, et al. Tracking progression with spectral-domain optical coherence tomography in geographic atrophy caused by age-related macular degeneration. *Invest Ophthalmol Vis Sci.* 51:3846–3852.
21. Helb HM, Issa PC, Fleckenstein M, et al. Clinical evaluation of simultaneous confocal scanning laser ophthalmoscopy imaging combined with high-resolution, spectral-domain optical coherence tomography. *Acta Ophthalmol.* 2010;88:842–849.
22. Pircher M, Gotzinger E, Findl O, et al. Human macula investigated in vivo with polarization-sensitive optical coherence tomography. *Invest Ophthalmol Vis Sci.* 2006;47:5487–5494.
23. Sarks JP, Sarks SH, Killingsworth MC. Evolution of geographic atrophy of the retinal pigment epithelium. *Eye (Lond).* 1988;2(pt 5):552–577.
24. Sarks S, Cherepanoff S, Killingsworth M, Sarks J. Relationship of basal laminar deposit and membranous debris to the clinical presentation of early age-related macular degeneration. *Invest Ophthalmol Vis Sci.* 2007;48:968–977.
25. Green WR, Key SN 3rd. Senile macular degeneration: a histopathologic study. *Trans Am Ophthalmol Soc.* 1977;75:180–254.
26. Green WR, Enger C. Age-related macular degeneration histopathologic studies: the 1992 Lorenz E. Zimmerman Lecture. *Ophthalmology.* 1993;100:1519–1535.
27. Sarks SH. Ageing and degeneration in the macular region: a clinicopathological study. *Br J Ophthalmol.* 1976;60:324–341.
28. Khanifar AA, Koreishi AF, Izatt JA, Toth CA. Drusen ultrastructure imaging with spectral domain optical coherence tomography in age-related macular degeneration. *Ophthalmology.* 2008;115:1883–1890.
29. Loffler KU, Lee WR. Basal linear deposit in the human macula. *Graefes Arch Clin Exp Ophthalmol.* 1986;224:493–501.
30. Marshall GE, Konstas AG, Reid GG, Edwards JG, Lee WR. Type IV collagen and laminin in Bruch's membrane and basal linear deposit in the human macula. *Br J Ophthalmol.* 1992;76:607–614.
31. van der Schaft TL, Mooy CM, de Bruijn WC, de Jong PT. Early stages of age-related macular degeneration: an immunofluorescence and electron microscopy study. *Br J Ophthalmol.* 1993;77:657–661.
32. Spraul CW, Lang GE, Grossniklaus HE, Lang GK. Histologic and morphometric analysis of the choroid, Bruch's membrane, and retinal pigment epithelium in postmortem eyes with age-related macular degeneration and histologic examination of surgically excised choroidal neovascular membranes. *Surv Ophthalmol.* 1999;44(suppl 1):S10–S32.
33. Curcio CA, Millican CL. Basal linear deposit and large drusen are specific for early age-related maculopathy. *Arch Ophthalmol.* 1999;117:329–339.
34. Starita C, Hussain AA, Pagliarini S, Marshall J. Hydrodynamics of ageing Bruch's membrane: implications for macular disease. *Exp Eye Res.* 1996;62:565–572.
35. Moore DJ, Clover GM. The effect of age on the macromolecular permeability of human Bruch's membrane. *Invest Ophthalmol Vis Sci.* 2001;42:2970–2975.
36. Hussain AA, Rowe L, Marshall J. Age-related alterations in the diffusional transport of amino acids across the human Bruch's-choroid complex. *J Opt Soc Am A Opt Image Sci Vis.* 2002;19:166–172.
37. Hillenkamp J, Hussain AA, Jackson TL, Cunningham JR, Marshall J. The influence of path length and matrix components on ageing characteristics of transport between the choroid and the outer retina. *Invest Ophthalmol Vis Sci.* 2004;45:1493–1498.